A&A 394, 707–715 (2002)
DOI: 10.1051/0004-6361:20021217

Astronomy & Astrophysics

Theoretical study of the collisional depolarization and of the Hanle effect in the Na I D_2 line observed on the solar limb

B. Kerkeni⋆ and V. Bommier

Laboratoire d'Étude du Rayonnement et de la Matière en Astrophysique, CNRS FRE 2460 – LERMA, Observatoire de Paris, Section de Meudon, 92195 Meudon, France

Received 31 May 2002 / Accepted 31 July 2002

Abstract. In recent years, Landi Degl'Innocenti (1998, 1999) has proposed a model of the polarization spectrum of the Na I D lines observed near the solar limb, based on lower level polarization effects. By so doing, he obtains a remarkable agreement between his model and the observations, so that he comes to a conclusion about a paradox, because the existence of lower level polarization is incompatible with a magnetic field strength higher than 10 mGauss (except vertical), and with possible depolarizing collision effects. In the present paper, we investigate the depolarizing collision effects (collisions with neutral hydrogen) by using the collisional rates computed with ab-initio and quantum chemistry methods by Kerkeni (2001; see also Kerkeni et al. 2000, and Kerkeni 2002). We solve the statistical equilibrium equations for the atomic density matrix, taking into account these depolarizing collisions. We investigate the effect of a weak magnetic field (Hanle effect). Our results indicate that the lower levels should be completely depolarized by the collisions at the depth where the Na I D lines are formed. Furthermore, large values of the lower level alignment such as those introduced by Landi Degl'Innocenti in his model to get a good theoretical fit of the observations, seem to us unlikely, as our computations confirm. Thus, as the agreement between the model by Landi Degl'Innocenti and the observations is however very convincing, the paradox is confirmed, reinforced and increased by our results.

Key words. Sun: atmosphere – Sun: magnetic fields – atomic data – atomic processes – line: formation – polarization

1. Introduction

The spectrum of the linear polarization of the Na I D lines observed near the solar limb is one of the most beautiful features of the second solar spectrum (which is the spectrum of the linear polarization observed near the solar limb). It has been observed several times in the recent years (Stenflo & Keller 1997; Keller & Sheeley 1999; Stenflo et al. 2000a, 2000b; Gandorfer 2000; Bommier & Molodij 2002). We will not discuss differences between these observations, in particular in the D_1 line polarization spectrum (peaked or not peaked). We are more interested in the remarkable interpretation of this spectrum proposed by Landi Degl'Innocenti (1998, 1999). What is remarkable in this interpretation is the agreement between the theoretical profile and the observations, which is highly convincing, but leads to a paradox.

The model proposed by Landi Degl'Innocenti (1998, 1999) is based on the following:

– the frequency coherent scattering is taken into account via a metalevels formalism (Landi Degl'Innocenti et al. 1997);
– the hyperfine structure of the Na I atom is taken into account, leading to a multi-level atomic scheme;
– the statistical equilibrium equations for the atomic density matrix are solved in the upper levels;
– a simplified treatment of the radiative transfer is formulated and used.

The model makes use of some free parameters. The lower level of the Na I D lines, $3^2S_{1/2}$, is split in two hyperfine levels $F = 1$ and $F = 2$, the nuclear spin being $I = 3/2$ (see Fig. 1). These two levels may show some atomic polarization or *alignment*, which results from unequal populations in the different Zeeman sublevels, though symmetrical sublevels M and $-M$ have equal populations. In the irreducible tensorial basis T^K_Q for developing the atomic density matrix in elements ${}^{FF}\rho^K_Q$, with $0 \leq K \leq 2F$ and $-K \leq Q \leq K$ (see Bommier 1995 for an introduction), the ${}^{FF}\rho^0_0$ element is proportional to the population of the F level (summed over the magnetic sublevels), and the ${}^{FF}\rho^2_0$ element is proportional to the alignment of the F level. The ratio ${}^{FF}\rho^2_0/{}^{FF}\rho^0_0$ is the atomic polarization. In the solar atmosphere where the upper level excitation is mainly radiative, alignment may be created in the upper level by absorption of anisotropic incident radiation. This upper level alignment can then be transferred to the lower level due to isotropic radiative spontaneous emission. Thus, the atomic polarization

Send offprint requests to: V. Bommier,
e-mail: V.Bommier@obspm.fr
⋆ *Present address*: Department of Chemistry, University College London, 20 Gordon Street, London UK-WC1H OAJ, UK
e-mail: b.kerkeni@ucl.ac.uk

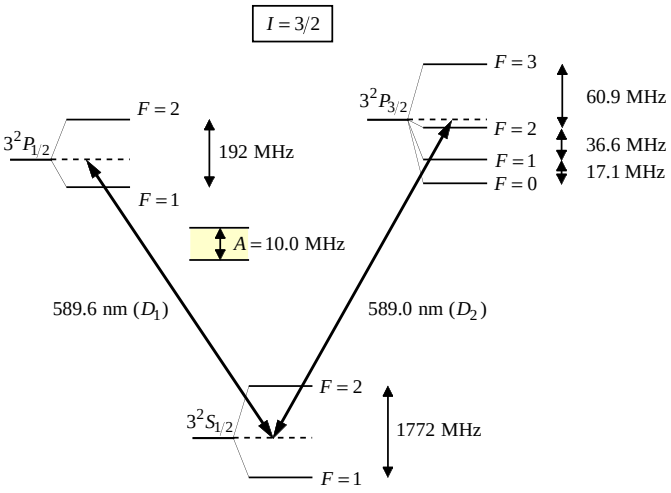

Fig. 1. Structure of the sodium atom, D lines. A is the Einstein emission coefficient (which is the same for the two D lines), ignoring the hyperfine structure (see Eq. (8)), expressed in MHz. It indicates the approximate natural width of the levels.

results from the anisotropy of the incident radiation, so that Landi Degl'Innocenti (1998, 1999) proposed the factorization

$$\frac{\rho^2_0}{\rho^0_0} = \beta w, \tag{1}$$

where w is the anisotropy of the incident radiation, defined as

$$w = \frac{J^2_0}{J^0_0}, \tag{2}$$

where J^0_0 and J^2_0 are the tensorial components of the incident radiation defined in Landi Degl'Innocenti (1984; see also Bommier 1997b, for a table of the irreducible spherical tensors for polarimetry that enter the definition of J^K_Q), and β is defined by Eq. (1). More recently (see Trujillo Bueno et al. 2002), it is rather used as the definition of w

$$w = \sqrt{2}\frac{J^2_0}{J^0_0}, \tag{3}$$

which has the advantage of leading to $-1/2 \leq w \leq 1$. β_1 and β_2, corresponding respectively to the two lower hyperfine levels $F = 1$ and $F = 2$, and w are three free parameters in Landi Degl'Innocenti's model. Another free parameter is the depth attenuation of β_1 and β_2 which is described with the parameter α (taking thus into account a possible collisional depolarization at large depth). The last free parameter is the Doppler broadening $\Delta\lambda_D$.

Landi Degl'Innocenti obtains a remarkable agreement of the theoretical polarization profile with the observation of Stenflo & Keller (1997), when non-zero values are introduced for the lower level alignment. The best agreement is obtained when $[\beta_1]_0 = 2.0$ and $[\beta_2]_0 = 3.8$, where $[\ ]_0$ means surface value. It is then concluded that the linear polarization spectrum is the result of non-zero lower level alignment. However, as it will be discussed below in more detail, the lifetime of the lower levels is such that the existence of non-zero alignment in the lower levels is incompatible with the existence of a magnetic field strength higher than 10 mGauss (except vertical), and is also incompatible with the existence of collisional depolarization. This may be considered as hardly believable, so that this result is a paradox.

More recently, on an observational basis, Stenflo et al. (2001) concluded that this lower level alignment effect could determine the D_1 polarization, but not the D_2 one which would rather result from upper level alignment and partial redistribution effects. This result is applied to the interpretation of new observations by Stenflo et al. (2002).

In the present paper, our purpose is to investigate the possible collisional depolarization of the lower level due to collisions of the sodium atom with neutral hydrogen atoms, by using recent collisional rates computed in the frame of abinitio and quantum chemistry calculations, by Kerkeni (2001; see also Kerkeni et al. 2000, and Kerkeni 2002). We solve the statistical equilibrium equations for the atomic density matrix, introducing these collisional depolarization rates. We obtain polarization in the D_2 line core by applying the last scattering approximation in the solar atmosphere. A zero magnetic field is assumed in Sect. 2, and the effect of the collisional depolarization on the Hanle effect of the D_2 line is investigated in Sect. 3. As a result, we derive the β_1 and β_2 coefficients at various depths of the chromosphere: we discuss this result in Sect. 4.

2. Collisional depolarization in a zero magnetic field

The aim of the present section is to investigate the effect of the depolarizing collisions on the scattering polarization of the Na I D_2 line, in a zero magnetic field as a first step. This is achieved by solving the statistical equilibrium equations for the atomic density matrix elements that fully describe the atomic polarization, in the last scattering approximation, for various values of the neutral hydrogen density. The data and the results of the statistical equilibrium equations are presented below.

2.1. Data for the statistical equilibrium equations

The statistical equilibrium equations for the atomic density matrix have been introduced by Bommier (1977; see also Bommier & Sahal-Bréchot 1978), were generalized to level-crossings in non-zero magnetic field in Bommier (1980), and to the case of an atom having a hyperfine structure like the sodium atom in Bommier & Sahal-Bréchot (1982). In the present work, the statistical equilibrium has been solved for the three levels involved in the Na I D lines, namely the ground level $3^2S_{1/2}$, the upper level of the Na I D_1 line $3^2P_{1/2}$, and the upper level of the Na I D_2 line $3^2P_{3/2}$ (see Fig. 1). The hyperfine structure ($I = 3/2$) has been taken into account, and the hyperfine level splittings for the sodium atom have been addressed in Sagalyn (1954).

In this formalism, the atomic density matrix is submitted to radiative excitation and de-excitation. The anisotropy and polarization of the incident radiation is described by means of an incident radiation density matrix that is coupled to the atomic density matrix in the radiative absorption and induced emission

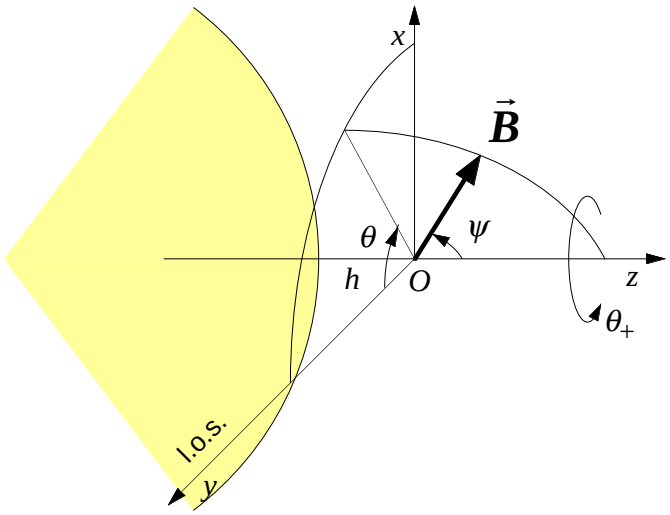

Fig. 2. Reference frame and angle definitions for the magnetic field vector (note that the azimuth θ angle is negative on the figure).

processes. The intensity of the incident radiation is described by means of dilution factors (see formalism and references in Bommier & Sahal-Bréchot 1978, and in Sahal-Bréchot 1974), in such a way that the incident radiation anisotropy w can be related to these dilution factors by

$$w = \frac{W_a}{W} \tag{4}$$

(in the definition of w given by Eq. (3)), where W_a is the anisotropic dilution factor and W is the total dilution factor. The emitted radiation polarization is described by means of an emitted photon density matrix, whose polarization state reflects that of the excited state of the line under interest.

The line absorption profiles are assumed to be narrower than the spectral variations of the incident radiation, which could eventually be questionable for the Na I D lines. Thus, the statistical equilibrium coefficients are integrated over these profiles, and the derived scattered polarization is the one at line center. As the D_1 line is unpolarizable, having $J = 1/2$ as the upper level angular momentum, because the hyperfine splittings are neglected in the calculation of the emissivity (let us recall that the hyperfine structure can only depolarize a line in such a case), we study the scattered linear polarization at the D_2 line center.

We have applied the last scattering approximation (Stenflo 1982): this approximation consists of assuming that the scattering atom is located just at the surface of the Sun, in such a way that the anisotropy of the incident radiation (which is assumed to be unpolarized) is given by the limb-darkening. The observed radiation results from the one-scattering of this incident radiation by the average atom. The symmetry axis of the incident radiation is the Oz axis of Fig. 2, and the emitted radiation is observed along the Oy axis of the same figure. The height above the solar limb h is then assumed to be zero.

The limb-darkening coefficient for the Na I D_2 line center has been derived from Waddel (1962): the intensity at the center of the Na I D_2 line, relative to the continuum intensity at disk center, observed at various disk center distances, has been fit by using the usual simple limb-darkening law

$$I(\vartheta)/I(0) = 1 - u + u\cos\vartheta, \tag{5}$$

where ϑ is the scattering angle (angle between the local solar radius and the line-of-sight). Thus, a value of $u = 0.255$ has been derived, leading to $w = 3.65 \times 10^{-2}$ for the incident radiation anisotropy.

The intensity of the incident radiation in the D_1 and D_2 line center has been taken in the solar atlas of Delbouille et al. (1973), as

$$\begin{aligned} I_{\min}(D_1) &= 5.0 \times 10^{-2} I_c \\ I_{\min}(D_2) &= 4.5 \times 10^{-2} I_c, \end{aligned} \tag{6}$$

where I_c is the continuum intensity at disk center, which is

$$I_c = 3.66 \times 10^{-5} \text{ erg cm}^{-2} \text{ s}^{-1} \text{ sr}^{-1} \text{ Hz}^{-1}, \tag{7}$$

at this wavelength. Thus, given the radiative emission probability

$$A_{21} = 0.629 \times 10^8 \text{ s}^{-1}, \tag{8}$$

which is the same for the two transitions $3^2P_{1/2} \rightarrow 3^2S_{1/2}$ (D_1) and $3^2P_{3/2} \rightarrow 3^2S_{1/2}$ (D_2), one obtains absorption probabilities that are three orders of magnitude smaller in the D line center:

$$\begin{aligned} B_{12} I_\nu(D_1) &= 0.61 \times 10^5 \text{ s}^{-1} \\ B_{12} I_\nu(D_2) &= 1.1 \times 10^5 \text{ s}^{-1}. \end{aligned} \tag{9}$$

Correlatively, the induced emission, that is fully taken into account in our computation, is in fact three orders of magnitude smaller than the spontaneous emission.

In the formalism described above, only radiative processes are considered. The purpose of the present paper is however to investigate the effect of the collisions with neutral hydrogen atoms on the lower and upper level polarization. These depolarizing collisions have been introduced in the statistical equilibrium equations following the formalism developed by Kerkeni (2002), in her Eqs. (16)–(18). Equation (16) is the statistical equilibrium equation for the atomic density matrix, taking into account the relaxation rates and also the collisional transition rates (that occur between the $3^2P_{1/2}$ and $3^2P_{3/2}$ levels), in the hyperfine and irreducible tensorial basis. In Eq. (17), the relaxation rates are developed on the hyperfine structure that plays no role during the collision, so that the hyperfine relaxation rates can be expressed in terms of the electronic relaxation rates $g^{KJ}(\lambda J)$ (Omont 1977). Equation (18) is the analogous development for the collisional hyperfine transition rates in terms of the electronic transfer rates $g^{KJ}(\lambda J, \lambda' J')$ from $\lambda' J'$ to λJ. The numerical values of the g^{KJ} rates used in the present work are slightly different from the ones given in Kerkeni (2002), because they correspond to fits in narrower temperature ranges, thus,

– level $3^2S_{1/2}$

$$g^1 = 4.32 \times 10^{-9} n_H \left(\frac{T}{5000}\right)^{0.41} \text{ s}^{-1} \tag{10}$$

(from Kerkeni et al. 2000);

– level $3^2P_{1/2}$

$$g^1 = 1.14 \times 10^{-8} n_H \left(\frac{T}{5000}\right)^{0.43} \text{ s}^{-1} \quad (11)$$

for 216 K $\leq T \leq$ 7000 K;

– level $3^2P_{3/2}$

$$g^1 = 9.90 \times 10^{-9} n_H \left(\frac{T}{5000}\right)^{0.43} \text{ s}^{-1}$$
$$g^2 = 1.17 \times 10^{-8} n_H \left(\frac{T}{5000}\right)^{0.44} \text{ s}^{-1}$$
$$g^3 = 1.14 \times 10^{-8} n_H \left(\frac{T}{5000}\right)^{0.44} \text{ s}^{-1} \quad (12)$$

for 1000 K $\leq T \leq$ 7000 K;

– transitions $3^2P_{1/2} \leftrightarrow 3^2P_{3/2}$

$$g^0(1/2 \rightarrow 3/2) = g^0(3/2 \rightarrow 1/2) = 5.84 \times 10^{-9} n_H \left(\frac{T}{5000}\right)^{0.45} \text{ s}^{-1} \quad (13)$$

for 216 K $\leq T \leq$ 7000 K,

$$g^1(1/2 \rightarrow 3/2) = g^1(3/2 \rightarrow 1/2) = -6.90 \times 10^{-10} n_H \left(\frac{T}{5000}\right)^{0.30} \text{ s}^{-1} \quad (14)$$

for 3000 K $\leq T \leq$ 7000 K. As for the fine structure collisional transition rate g, one has

$$g(1/2 \rightarrow 3/2) = \sqrt{2} g^0(1/2 \rightarrow 3/2) \quad (15)$$

and

$$g(3/2 \rightarrow 1/2) = \frac{1}{\sqrt{2}} g^0(3/2 \rightarrow 1/2). \quad (16)$$

2.2. Results of the statistical equilibrium

The results of the statistical equilibrium are given in Fig. 3, in which the scattered linear polarization rate is given as a function of the neutral hydrogen density.

The obtained polarization degree has an order of magnitude compatible with the one observed at the D_2 line center near the solar limb (see the results of observations in Stenflo & Keller 1997; Keller & Sheeley 1999; Stenflo et al. 2000a, 2000b; Gandorfer 2000; Bommier & Molodij 2002). The observations are however performed inside the solar limb (except the ones of Keller & Sheeley 1999, which are very close to the limb and give a polarization rate of the order of 5×10^{-3} at D_2 line center), whereas the present calculation is a crude model that corresponds to a scattering point that would be located exactly on the limb. It has to be kept in mind that the polarization degree decreases rapidly when the limb distance increases.

The linear polarization rate decreases when the density increases, in two steps: first, for $10^{12} \leq n_H \leq 10^{14}$, the alignment (or atomic polarization) is being progressively destroyed

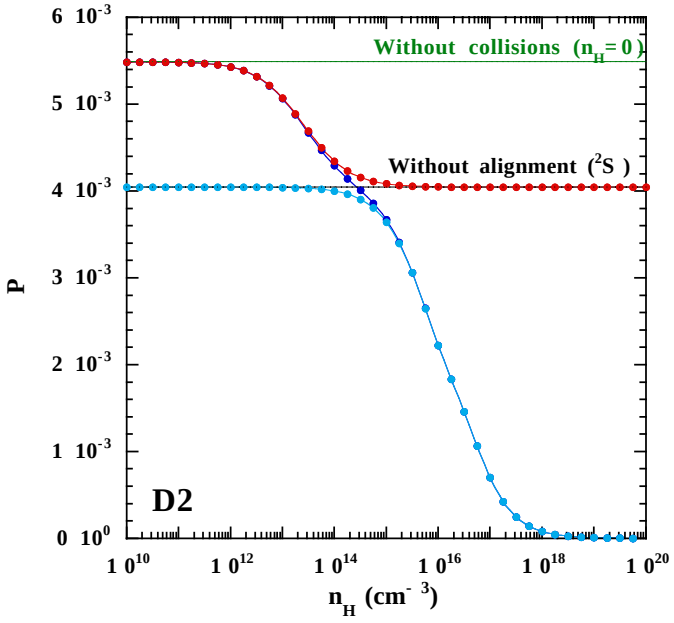

Fig. 3. Collisional depolarization of the Na I D_2 line: linear polarization rate at line center P, as a function of the neutral hydrogen density n_H. The upper horizontal line, at $P = 5.49 \times 10^{-3}$, represents the polarization scattered without any collision, taking into account the lower levels polarization. The lower horizontal line, at $P = 4.04 \times 10^{-3}$, represents the polarization scattered without any collision also, but assuming unpolarized lower levels. The right curve that decreases from $P = 5.49 \times 10^{-3}$ to $P = 4.04 \times 10^{-3}$ is obtained when the depolarizing collisions are introduced in the lower levels only. The left curve that decreases from $P = 4.04 \times 10^{-3}$ to $P = 0$ is obtained when the depolarizing collisions are introduced in the upper levels, and the lower levels are assumed to be unpolarized. The composite "central" curve that decreases from $P = 5.49 \times 10^{-3}$ to $P = 0$ is the general curve that is obtained when the depolarizing collisions are introduced in both upper and lower levels.

in the lower hyperfine levels. These levels, having as total angular momentum $F = 1$ and $F = 2$ (see Fig. 1), may be polarized. Then, for $10^{15} \leq n_H \leq 10^{17}$, the alignment (or atomic polarization) is being progressively destroyed in the upper levels. The alignment is partly destroyed when the relaxation rates are of the same order of magnitude as the level inverse lifetime (totally destroyed if the relaxation rates are higher than the inverse lifetime). It can be seen above (Eqs. (10)–(14)) that all the relaxation rates have the same order of magnitude, in the lower as well as in the upper levels. As the lifetime is three orders of magnitude longer in the lower levels than in the upper levels, as dicussed above, the depolarizing densities differ by three orders of magnitude for these two series of levels, as is visible in Fig. 3.

As will be discussed later, the neutral hydrogen density at the Na I D line formation depth which is located near the temperature minimum is of the order of 2×10^{15} cm^{-3} (temperature minimum, model C for the Quiet Sun by Fontenla et al. 1993), so that, following our result given in Fig. 3, the lower level polarization would be completely destroyed at this depth, whereas the upper level polarization would not be destroyed. This point will be further investigated in Sect. 4.

3. Hanle effect and collisional depolarization

Here we investigate the effect of a weak magnetic field on the Na I D_2 line scattering polarization. A weak magnetic field, when aligned with the line-of-sight in the scattering geometry of Fig. 2, is able to decrease the linear polarization rate, and to rotate the linear polarization direction with respect to the solar limb direction (which is the polarization direction in a zero magnetic field): these are the two main features of the Hanle effect.

The effect of the magnetic field on the hyperfine sublevel energy is given in Fig. 4. On this figure, it can be seen that level-crossings and anti-level-crossings occur between the hyperfine sublevels of the upper level $3^2P_{3/2}$ of the Na I D_2 line, for a field strength lower than 60 Gauss. The transition from the Zeeman effect to the Back-Goudsmit effect, where the hyperfine hamiltonian is smaller than the electron-magnetic field interaction hamiltonian, is clearly visible on the figure. The result is that, for such a magnetic field strength, the nuclear angular momentum becomes decoupled from the electronic angular momentum (Casini et al. 2002), so that the hyperfine structure becomes negligible.

We have investigated the magnetic field effect for three typical neutral hydrogen densities:

- zero neutral hydrogen density (collisionless regime);
- $n_{\rm H} = 2 \times 10^{14}$ cm^{-3}: for this density, the atomic polarization is destroyed in the lower levels and not destroyed in the upper levels (see Fig. 3);
- $n_{\rm H} = 10^{16}$ cm^{-3}: for this density, the atomic polarization is destroyed in the lower levels and partially destroyed also in the upper levels (see Fig. 3).

The Hanle diagrams have been plotted for these three densities in Figs. 5–7 respectively. These diagrams are abaci of the linear polarization in rate and direction, for an horizontal magnetic field ($\psi = 90°$), and for various field strengths B and azimuths θ.

The diagram for the zero neutral hydrogen density has already been computed by Landolfi & Landi Degl'Innocenti (1985), in the solar prominences case (i.e. at a higher altitude above the solar limb). However, when scaled to the linear polarization rate in zero magnetic field $p_{\rm max}$, the diagram practically does not depend on the scattering height, so that our diagram given in Fig. 5 is in good agreement with the one given in Fig. 4 of Landolfi & Landi Degl'Innocenti (1985). Three main features can be described on this diagram.

The first feature concerns the incomplete loop that is visible at the top of the diagram. This loop is the result of the progressive destruction of the atomic coherences responsible for the lower levels polarization by the increasing magnetic field (the upper levels coherences are destroyed at a higher magnetic field strength). More precisely, the coherences are completely destroyed when $\omega\tau \gg 1$, where ω is the Larmor frequency and τ the lifetime of the level under interest, so that the average Hanle sensitivity of the polarization to the magnetic field strength is given by $\omega\tau = 1$. For the lower level $3^2S_{1/2}$, the lifetime being given by the radiative absorption probabilities given in Eq. (9), this corresponds to a field strength of 5–10 mGauss for the Hanle sensitivity. For the upper level $3^2P_{3/2}$, the lifetime is given by the radiative emission probability given in Eq. (8), and this corresponds to a field strength of 5 Gauss for the Hanle sensitivity (three orders of magnitude higher because the lifetime

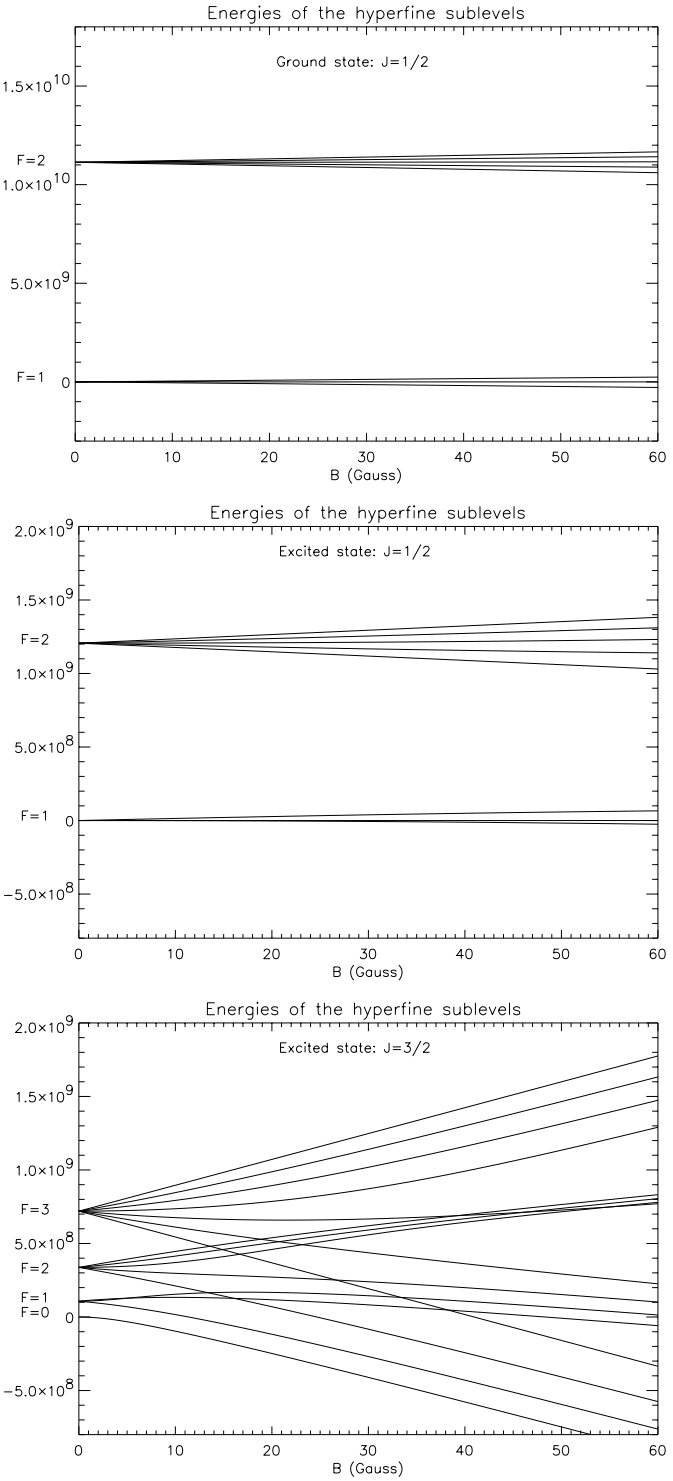

Fig. 4. Effect of the magnetic field on the hyperfine structure sublevels energies, for the levels $3^2S_{1/2}$ (ground level, top), $3^2P_{1/2}$ (excited level of the Na I D_1 line, middle), and $3^2P_{3/2}$ (excited level of the Na I D_2 line, bottom). The energies (y-axis) are given in angular frequency units, rad/s. On the bottom figure, the transition from the Zeeman effect to the Back-Goudsmit effect appears clearly.

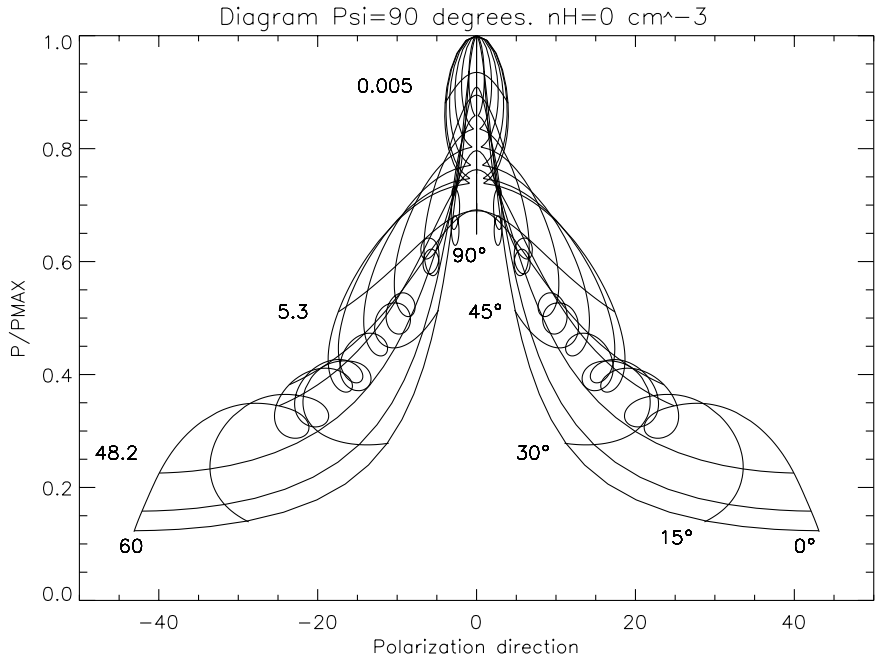

Fig. 5. Hanle effect diagram for an horizontal magnetic field ($\psi = 90°$). x-axis: linear polarization direction with respect to the solar limb direction (x-axis of Fig. 2). y-axis: linear polarization rate at Na I D_2 line center (scaled to the linear polarization rate in zero magnetic field, $p_{\max}$). The vertically oriented curves are iso-θ curves (increasing field strength and constant field azimuth – some θ values are given near the bottom extremity). The horizontally oriented curves are iso-gauss curves (constant field strength and varying field azimuth – some B values in Gauss are given near the left extremity). The loops are associated to some Zeeman sublevel crossings (see text). For this diagram, a zero neutral hydrogen density has been assumed, and $p_{\max} = 5.49 \times 10^{-3}$. The height above the solar limb is zero and the anisotropy of the incident radiation results from the limb darkening (see text).

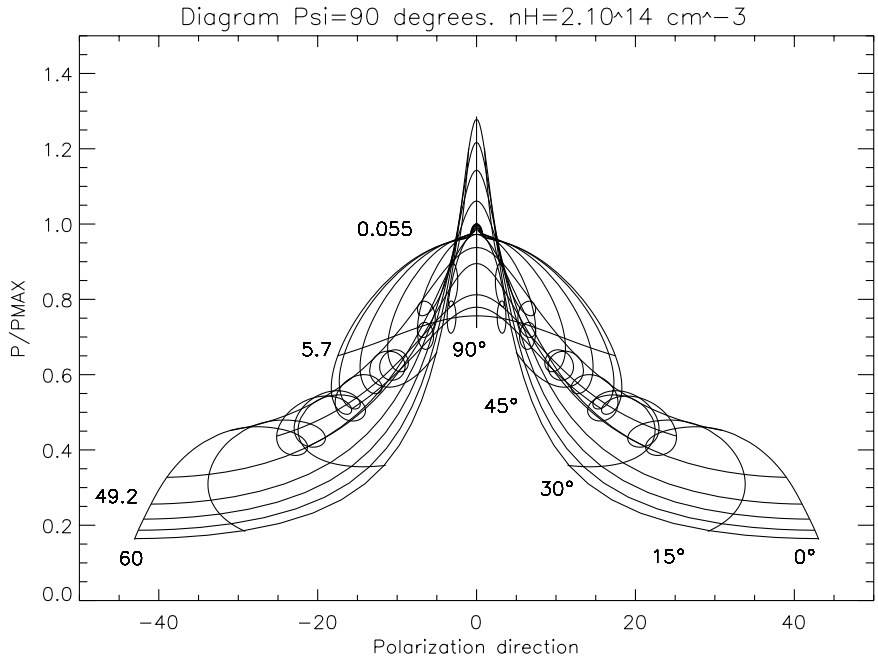

Fig. 6. Same as Fig. 5, but for a neutral hydrogen density of 2×10^{14} cm^{-3}. For such a density, the lower levels are depolarized by the collisions with neutral hydrogen (see Fig. 3). $p_{\max} = 4.11 \times 10^{-3}$.

is three orders of magnitude smaller in the upper level than in the lower level). These two widely different ranges of field strengths are clearly visible on the diagram: the smaller field, 5 mGauss, is associated to the incomplete loop corresponding to the lower level polarization progressive destruction.

The second feature concerns the small loops that appear at field strength in the 10–20 Gauss range (two loops on each iso-θ curve). As discussed in Bommier (1980), such loops are associated with level-crossings (having $\Delta M = \pm 2$ for the magnetic quantum number difference between the two crossing levels, due to symmetry reasons for horizontal magnetic field having $\psi = 90°$), that appear in the lower part of Fig. 4. Three level-crossings having $\Delta M = \pm 2$ can be found in this figure, in the range 15–25 Gauss, corresponding to these two loops.

The third feature concerns the increase of polarization rate for high fields, for azimuths θ around 90°. This increase is more visible on the top curve of Fig. 8, where we have plotted the variation of the polarization rate as a function of the magnetic field strength, for horizontal field $\psi = 90°$ having also azimuth $\theta = 90°$ (magnetic field lying along the Ox axis of Fig. 2). On this curve we can also see the two other features: the lower level depolarization for field strength in the range 5–10 mGauss, and two small bumps corresponding to the loops that appear for the other azimuths (for this azimuth, $\theta = 90°$, due to symmetry reasons there is no rotation of the polarization direction). This increase of polarization, already observed in the computations by Trujillo Bueno et al. (2002), is due to the decoupling of the nuclear angular momentum from the

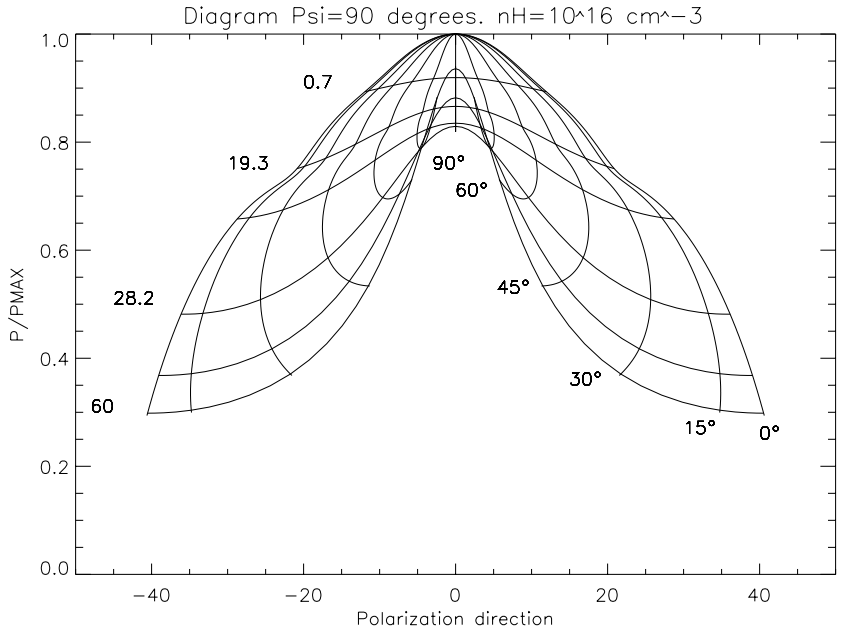

Fig. 7. Same as Fig. 5, but for a neutral hydrogen density of 1×10^{16} cm^{-3}. For such a density, the lower levels are totally depolarized and the upper levels are partly depolarized also by the collisions with neutral hydrogen (see Fig. 3). Moreover, the upper levels are broadened by the collisions, which explains the disappearance of the loops (see text). $p_{\max} = 2.22 \times 10^{-3}$.

electronic angular momentum (Casini et al. 2002), or, in other words, to non-zero coherences in the atomic density matrix between levels having different total quantum numbers $F \neq F'$. When the nuclear angular momentum is decoupled, the hyperfine structure, which has a depolarizing effect, becomes negligible, so that the polarization increases.

The symmetries of the problem that are discussed in Bommier (1980) imply that two symmetries are visible in Figs. 5–7: first, two opposite azimuths $+\theta$ and $-\theta$ correspond to the same polarization degree and direction; second, two complementary azimuths θ and $\pi - \theta$ correspond to the same polarization degree but opposite polarization direction rotations.

Figure 6 corresponds to the diagram modified by the depolarizing collisions, when a neutral hydrogen density $n_{\rm H} = 2 \times 10^{14}$ cm^{-3} is assumed. As can be seen in Fig. 3, such a density corresponds to the case where the polarization is destroyed in the lower levels, but not in the upper levels. Thus, the incomplete loop that was visible at the top of the diagram in the collisionless regime (Fig. 5), that was associated with the progressive destruction of the coherences in the lower level, is no longer visible in Fig. 6 because the lower level coherences are destroyed by the collisions, whatever the field strength. The two other features (loops corresponding to level-crossings and increase of the polarization for high field strength) are also visible in this diagram and in the corresponding middle curve of Fig. 8. Due to the disappearance of the incomplete top loop, the increase of polarization due to the nuclear angular momentum decoupling is clearly visible, and corresponds to a polarization degree higher than the one in a zero magnetic field, $p_{\max}$.

Figure 7 corresponds to the diagram modified by the depolarizing collisions, when a neutral hydrogen density $n_{\rm H} = 10^{16}$ cm^{-3} is assumed. As it can be seen in Fig. 3, such a density corresponds to the case where the polarization is totally destroyed in the lower level, and partly destroyed in the upper level. As in the preceding case, the incomplete top loop due to the lower level coherences is not visible, because the lower

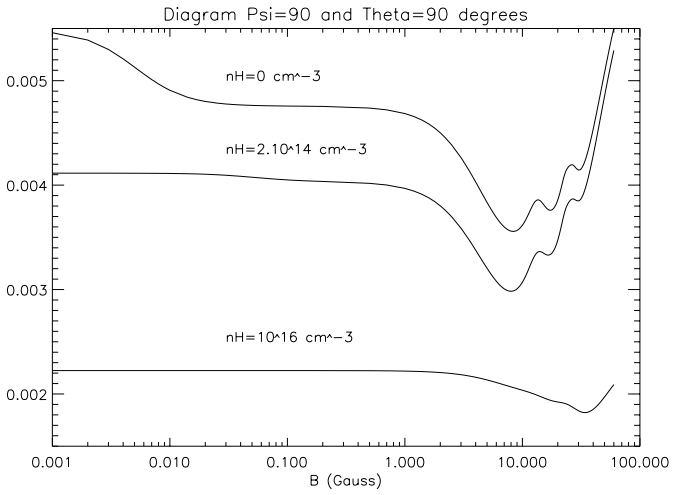

Fig. 8. Variation of the linear polarization rate (y-axis, not scaled to a zero field value as the Hanle diagrams) with increasing magnetic field strength, for an horizontal field $\psi = 90°$, with azimuth $\theta = 90°$ (field aligned with the x-axis of Fig. 2), for the three neutral hydrogen densities considered for plotting the Hanle diagrams given in Figs. 5–7.

level polarization is completely destroyed by the collisions. The two other features (loops corresponding to level-crossings and increase of the polarization for high field strength) are also not or much less visible on this diagram. This is due to the fact that, besides their depolarizing effect, the collisions have a broadening effect which makes the associated level width larger that the hyperfine splitting, so that the hyperfine structure (responsible for the level-crossings) becomes negligible whatever the magnetic field strength is. A similar effect of negligible hyperfine structure with respect to the upper level width has already been studied in the case of the hydrogen Lyα line scattered in the solar Corona, by Bommier & Sahal-Bréchot (1982).

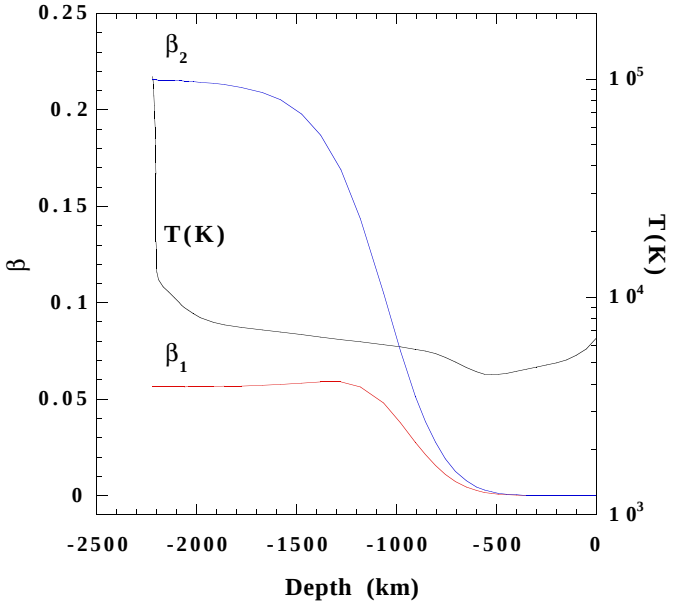

Fig. 9. Beta coefficients (see text), that describe the lower levels alignment, for the two hyperfine lower levels $F = 1$ and $F = 2$ (left y-axis), as a function of the depth in the chromosphere. The electron temperature (right y-axis) is also given. The Na I D lines are formed near the temperature minimum.

4. Discussion

The aim of the present section is to investigate the dependence of the lower level polarization on the depth in the chromosphere. The lower level polarization is described by the β coefficient introduced in Eq. (1). We have computed the β_1 and β_2 coefficients corresponding to the two hyperfine lower levels $F = 1$ and $F = 2$ respectively, by solving the statistical equilibrium equations under the conditions described in the preceding Sect. 2.1. In particular, the incident radiation anisotropy is that resulting from the last scattering approximation, as if the scattering atom was located at the Sun's surface. This anisotropy is certainly different from the one deeper in the chromosphere. However, we estimate that the factorization introduced in Eq. (1) is such that the β coefficient does not depend on the anisotropy of the incident radiation (which is factorized in the w coefficient), so that our solution of the statistical equilibrium equation may provide the $\beta_{1,2}$ coefficients at any chromosphere depth.

We have used the neutral hydrogen density values given as a function of depth by the Quiet Sun model C of Fontenla et al. (1993).

The derived $\beta_{1,2}$ coefficients as a function of chromosphere depth are given in Fig. 9. Two main conclusions can be drawn from this figure.

The first conclusion is that our $\beta_{1,2}$ coefficients remain substantially smaller than unity at any depth, unlike the large values introduced by Landi Degl'Innocenti in his model to get a good theoretical fit of the observations (see Sect. 1). We estimate that such a behavior of the β coefficients as the one we obtain is to be expected, because the only source of anisotropy in the statistical equilibrium equations is the incident radiation anisotropy. If Eq. (2) is used to define the w coefficient, β should thus remain ≤ 1, whereas it should remain $\leq 1/\sqrt{2}$ (as we obtain in our computation) if Eq. (3) is used instead to define w.

The second conclusion is that the $\beta_{1,2}$ coefficients are very small, so that the lower levels are unpolarized, near the temperature minimum where the Na I D lines are expected to form.

5. Conclusion

The result of our solution of the statistical equilibrium equations for the atomic density matrix, taking into account the depolarizing collisions with neutral hydrogen through the collisional rates computed by Kerkeni (2001; see also Kerkeni et al. 2000, and Kerkeni 2002), is that the lower levels of the Na I D lines would be completely depolarized near the temperature minimum where the Na I D lines are expected to form. In his model of the Na I D lines scattering polarization, Landi Degl'Innocenti (1998, 1999) obtains a remarkable agreement with the observations of Stenflo & Keller (1997), if on the contrary a large value is assumed for the lower level alignment (or polarization). As this alignment could be destroyed by the depolarizing collisions (that we confirm) or by a magnetic field larger than 5–10 mGauss (except vertical), he came to a conclusion about a paradox. Our conclusion based on our computations of the depolarizing collisions effect confirm, reinforces and increases the paradox.

The values of the β coefficients for the lower levels introduced by Landi Degl'Innocenti in his model to get a good theoretical fit of the observations are larger than unity. We estimate, and our computations confirm, that such large values are unlikely, because the only source of anisotropy is the incident radiation one, so that β should remain ≤ 1 (if Eq. (2) is used to define the incident radiation anisotropy coefficient w), or $\leq 1/\sqrt{2}$ (if Eq. (3) is used instead). This also increases the paradox.

The modelling of the Na I D lines remains unresolved, difficult to solve because several important effects are involved and mixed, namely: frequency coherent scattering, a multi-level atom (due to the hyperfine structure), and polarized radiative transfer. As a preliminary step, our statistical equilibrium code could be improved by implementation of the line profiles, following the formalism developed by Bommier (1997a, 1997b), in order to allow spectral variations of the incident radiation along the absorption profile.

References

Bommier, V. 1977, Thèse de troisième cycle, Paris VI University
Bommier, V. 1980, A&A, 87, 109
Bommier, V. 1995, SPW1 Proc., St Petersburg (also Sol. Phys., 164, 29)
Bommier, V. 1997a, A&A, 328, 706
Bommier, V. 1997b, A&A, 328, 726
Bommier, V., & Sahal-Bréchot, S. 1978, A&A, 69, 57
Bommier, V., & Sahal-Bréchot, S. 1982, Sol. Phys., 78, 157
Bommier, V., & Molodij, G. 2002, A&A, 381, 241
Casini, R., Landi Degl'Innocenti, E., Landolfi, M., & Trujillo Bueno, J. 2002, ApJ, 573, 864

Delbouille, L., Roland, G., & Neven, L. 1973, Photometric atlas of the solar spectrum from $\lambda = 3000$ to $\lambda = 10\,000$, Université de Liège, Institut d'Astrophysique (ed.)
Fontenla, J. M., Avrett, E. H., & Loeser, R. 1993, ApJ, 406, 319
Gandorfer, A. 2000, The Second Solar Spectrum, a high spectral resolution polarimetric survey of scattering polarization at the solar limb in graphical representation (Hochschulverlag AG an der ETH Zürich)
Keller, C. U., & Sheeley, N. R. Jr. 1999, Proc. of the 2nd Solar Polarization Workshop, ed. K. N. Nagendra, & J. O. Stenflo, ASSL Ser. 243 (Kluwer, Dordrecht), 17
Kerkeni, B. 2001, Thèse de doctorat, Paris VI University
Kerkeni, B. 2002, A&A, 390, 783
Kerkeni, B., Spielfiedel, A., & Feautrier, N. 2000, A&A, 358, 373 and 364, 937
Landi Degl'Innocenti, E. 1984, Sol. Phys., 91, 1
Landi Degl'Innocenti, E. 1998, Nature, 392, 256
Landi Degl'Innocenti, E. 1999, Proc. of the 2nd Solar Polarization Workshop, ed. K. N. Nagendra, & J. O. Stenflo, ASSL Ser., 243 (Kluwer, Dordrecht), 61
Landi Degl'Innocenti, E., Landi Degl'Innocenti, M., & Landolfi M. 1997, in Forum THEMIS, La science avec THEMIS, Science with THEMIS, proceedings of a meeting held in Meudon (France), 1996 November 14–15, ed. N. Mein, & S. Sahal-Bréchot (Paris Observatory publ.), 59
Landolfi, M., & Landi Degl'Innocenti, E. 1985, Sol. Phys., 98, 53
Omont, A. 1977, Prog. Quant. Electron., 5, 69
Sagalyn, P. L. 1954, Phys. Rev., 94, 885
Sahal-Bréchot, S. 1974, A&A, 36, 355
Stenflo, J. O. 1982, Sol. Phys., 80, 209
Stenflo, J. O., & Keller, C. U. 1997, A&A, 321, 927
Stenflo, J. O., Gandorfer, A., & Keller, C. U. 2000a, A&A, 355, 781
Stenflo, J. O., Keller, C. U., & Gandorfer, A. 2000b, A&A, 355, 789
Stenflo, J. O., Gandorfer, A., Wenzler, T., & Keller, C. U. 2001, A&A, 367, 1033
Stenflo, J. O., Gandorfer, A., Holzreuter, R., et al. 2002, A&A, 389, 314
Trujillo Bueno, J., Casini, R., Landolfi, M., & Landi Degl'Innocenti, E. 2002, ApJ, 566, L53
Waddel, J. 1962, ApJ, 136, 223